Advances in Natural
Sciences: Nanoscience
and Nanotechnology

PAPERS • OPEN ACCESS

Mulberry leaf extract mediated synthesis of gold nanoparticles and its anti-bacterial activity against human pathogens

To cite this article: K Adavallan and N Krishnakumar 2014 *Adv. Nat. Sci: Nanosci. Nanotechnol.* **5** 025018

View the article online for updates and enhancements.

You may also like

- Electrostatic effect of Au nanoparticles on near-infrared photoluminescence from Si/SiGe due to nanoscale metal/semiconductor contact
Yefei Yin, Ze Wang, Shuguang Wang et al.
- Restoration of ampicillin susceptibility in drug-resistant *enterococcus faecalis* via synergistic therapy with co-functionalized gold nanoparticles
Qingqing Li, Mingzhi Huang and Peng Wang
- Facile preparation of surfactant-free Au NPs/RGO/Ni foam for degradation of 4-nitrophenol and detection of hydrogen peroxide
Y Y Liu, X L Guo, L Zhao et al.

This content was downloaded from IP address 15.204.172.50 on 09/11/2026 at 11:14

OPEN ACCESS

IOP Publishing | Vietnam Academy of Science and Technology

Advances in Natural Sciences: Nanoscience and Nanotechnology

Adv. Nat. Sci.: Nanosci. Nanotechnol. **5** (2014) 025018 (9pp)

doi:10.1088/2043-6262/5/2/025018

Mulberry leaf extract mediated synthesis of gold nanoparticles and its anti-bacterial activity against human pathogens

K Adavallan and N Krishnakumar[1]

Department of Physics, Annamalai University, Annamalainagar 608 002, Tamil Nadu, India

E-mail: nskumarphyamu@gmail.com

Received 1 October 2013
Accepted for publication 14 April 2014
Published 13 May 2014

Abstract

Gold nanoparticles (Au-NPs) were synthesized at room temperature using *Morus alba* (mulberry) leaf extract as reducing and stabilizing agent. The development of plant mediated synthesis of nanoparticles is gaining importance due to its simplicity, low cost, non-toxicity, eco-friendliness, long term stability and reproducible aqueous synthesis method to obtain a self-assembly of nearly monodispersed Au-NPs. The formation and morphology of biosynthesized nanoparticles are investigated with the help of UV-Vis spectroscopy, dynamic light scattering (DLS), transmission electron microscopy (TEM), atomic force microscopy (AFM), x-ray diffraction (XRD), and Fourier transform infrared spectroscopy (FT-IR) techniques. Au-NPs formation was screened by UV-Vis spectroscopy through color conversion due to surface plasmon resonance band at 538 nm for Au-NPs. DLS studies revealed that the average size of Au-NPs was 50 nm. TEM studies showed the particles to be nearly spherical with few irregular shapes and particle size ranges 15–53 nm. The AFM image clearly shows the surface morphology of the well-dispersed Au-NPs with less than 50 nm. The high crystallinity of nanoparticles is evident from bright circular spots in the selected area electron diffraction (SAED) pattern. X-ray diffraction pattern showed high purity and face-centered cubic structure of Au-NPs. The FT-IR results indicate the presence of different functional groups present in the biomolecule capping the nanoparticles. Further, biosynthesized Au-NPs show strong zone of inhibition against *Vibrio cholera* (gram-negative) and *Staphylococcus aureus* (gram-positive) whereas, chemically synthesized Au-NPs and mulberry leaf extract exhibit a fair zone of inhibition.

Keywords: gold nanoparticles, biosynthesis, mulberry leaf, anti-bacterial activity
Classification numbers: 2.05, 4.02

1. Introduction

Nanotechnology is emerging as a rapidly growing field with its applications in industrial, biomedical and electronic applications. Nanoparticles of noble metals belong to the most extensively studied colloidal systems in the field of nanoscience and nanotechnology. Noble metals such as Au, Ag, Pd, Pt and Cu have been widely used for the synthesis of stable colloids which are useful in the areas of optoelectronics [1], catalysis [2], photothermal therapy [3], surface enhanced Raman scattering (SERS) detection [4] and biological labelling [5]. Among several metal nanoparticles, gold nanoparticles (Au-NPs) have been considered an important area of research due to their unique and intense plasmon resonance in the visible range and their applications in biomedical field. Synthesis of Au-NPs by chemical methods leads to the presence of some toxic chemical species adsorbed on the surface that may have adverse effects in medical applications [6]. Due to the obvious disadvantages of the chemical reduction method, a biological synthesis method has been developed to obtain biocompatible, inexpensive and eco-friendly size controlled nanoparticles [7]. Biological route synthesis of

[1] Author to whom any correspondence should be addressed.

 © 2014 Vietnam Academy of Science & Technology

Original content from this work may be used under the terms of the Creative Commons Attribution 3.0 licence. Any further distribution of this work must maintain attribution to the author(s) and the title of the work, journal citation and DOI.

nanoparticles has received much focused attention from researchers in order to elucidate the mechanism of synthesis. Nowadays bioreduction methods based on fungi, microorganisms and plant extracts are being attempted due to the ease of synthesis, environmentally benign nature and greater stability of nanoparticles [8]. In recent years, plant materials have been of special interest to the scientific community due to their eco-friendliness and are advantageous over other biological processes because they eliminate the elaboration of the process of maintaining cell structures and can also be suitably scaled up for large scale synthesis of nanoparticles [9]. Reduction of Au^{3+} using plant extracts is advantageous since the phytochemicals have several medicinal properties which may aid in therapy and may be superior to polymer capped Au-NPs. Recently, the synthesis of Au-NPs has been reported using plants such as, *Chenopodium album* [10], *Ocimum sanctum* [11], *Cassia auriculata* [12], *Rosa hybrida* [13], *Crocus sativus* [14], *Rosa damascena* [15], *Thuja orientalis* [16], *Terminalia chebula*. [17] Ankamwar *et al* [18] reported the synthesis of gold nanotriangles using tamarind leaf extract and studied their potential applications in vapor sensing. Govindaraju *et al* [19] demonstrated the *β*-glucosidase assisted biosynthesis of Au-NPs and this report also focused on the newly formed Au-NPs application on promoting the defensive mechanism of silkworm *Bombyx mori*. Banker *et al* [20] investigated banana peel extract mediated Au-NPs displaying efficient anti-microbial activity towards most of the tested fungal and bacterial cultures. Daizy *et al* [21] reported that *Cassia fistula* stem bark mediated Au-NPs are better hypoglycemic agents in the treatment of diabetes mellitus and its associated complications. Mukherjee *et al* [22] proposed that green synthesized gold nanobioconjugates using *Olax Scandens* leaf (Au-NPs-OX) could be used as alternative diagnostic and therapeutic approaches for cancer diseases. Kumar *et al* [23] reported that the physicochemical properties, biostability and blood compatibility evaluation of Au-NPs prepared from *Zingiber officinale* extract support its usage as vectors for the applications in drug delivery, gene delivery or as biosensors, where a direct contact with blood occurs. Fayaz *et al* [24] have reported that the synthesized gold nanotriangles using *Maduca longifolia* leaf extract can be easily coated in the glass windows which are highly efficient in absorbing IR radiations.

Genus *Morus* (mulberry) is one such example that consists of over 150 species; among them *Morus alba L.* is dominant [25]. Mulberry leaf (the leaf of *Morus alba*) commonly used in the silkworm diet, has been used in edible foods. Dietary mulberry (*Morus alba*) leaf exhibits a wide range of pharmacological effects such as anti-microbial antioxidant anti-inflammatory functions, activity against atherosclerosis and diabetes mellitus, neuroprotective functions and L-3,4-dihydroxyphenylalanine (DOPA) oxidase inhibition and antityrosinase activity [26]. It has a unique nutritional profile containing proteins, phenolics, flavonoids and anthocyanins that enhances its significance as promising nature's functional tonic [27]. The polyphenols contained in mulberry leaf also show the ability to inhibit cancer cell proliferation, invasion, and metastasis [28]. Also, mulberry leaves are rich in iminosugars such as the glucose analogue 1-deoxynojirimycin (DNJ), *N*-methyl-DNJ, and 2-*O*-*α*-D-galactopyranosyl-DNJ, DNJ being the most abundant and accounting for 50% of the mulberry iminosugars [29]. Since DNJ is believed to be the most bioactive agent (R-glucosidase inhibitor), dietary mulberry DNJ might be beneficial for suppressing abnormally high blood glucose levels, thereby helping to prevent diabetes mellitus. At present, various food-grade mulberry products (i.e., teas, powders, and tablets) have been made commercially available in Japan and many other countries [30]. So far, there is no report on the synthesis of Au-NPs by utilizing the aqueous leaf extract of *Morus alba.* Hence, the present study involves the synthesis and characterization of mulberry leaf (*Morus alba*) mediated Au-NPs and evaluating the anti-bacterial effect of biosynthesized Au-NPs in comparison to chemically synthesized Au-NPs and plant extract against human pathogens such as *Staphylococcus aureus* (gram-positive) and *Vibrio cholera* (gram-negative) bacteria.



Figure 1. Photograph of *Morus Alba* leaf.

2. Materials and methods

2.1. Materials

The mulberry *(Morus alba L.)* leaves (figure 1) were obtained from Sericulture Farmers Training Centre at Jayankondapattinam, Tamilnadu, India. Hydrogen tetra chloroaurate (III) hydrate ($HAuCl_4$. 3 H_2O) was purchased from Sigma-Aldrich Chemicals, Bangalore, India and used as-received. Nutrient agar for bacterial culture and Muller–Hinton broth and agar for anti-bacterial activity were purchased from Hi-Media, Mumbai, India. All other reagents used in the reaction were of analytical grade with maximum purity. All aqueous solutions were prepared using de-ionized water. All glasswares were cleaned with chromic acid followed by thorough washing with de-ionized water and then acetone for prior use.

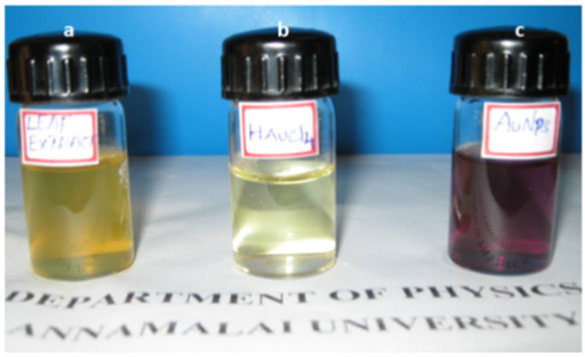


Figure 2. Photograph of colloids (a) *Morus alba* leaf extract, (b) 10^{-4} M $HAuCl_4$ metal ion solution and (c) purple pink color indicating the formation of Au-NPs.

2.2. Preparation of leaf extracts

The fourth and fifth leaves from the apex of the healthy plants were plucked and washed with de-ionized water until no foreign material remained. The leaves were shade-dried for 5 days and ground into fine powder using an electrical blender. The powdered samples were stored in an air tight container and protected from sunlight for further use. 10 g of leaf powder was taken and mixed with 100 ml of de-ionized water and kept in a boiling water bath at 60 °C for 15 min. The extracts were filtered with Whatman filter paper no. 1. The filtered extract was stored in a refrigerator for further experiments as reducing agent and stabilizer.

2.3. Chemical synthesis of gold nanoparticles

Au-NPs with an approximate diameter of 20 nm were synthesized using the modified Turkevich method [31]. Briefly, 30 mL of 0.25 mM $HAuCl_4$ solution was added to Erlenmeyer flasks and heated to 80 °C. Once a stable temperature was achieved, Au^{3+} solution was reduced by adding 1.5 mL of 1% sodium citrate solution. The solution was maintained at that temperature until the solution turned ruby red, indicating Au-NPs had formed.

2.4. Biosynthesis of gold nanoparticles

For the biosynthesis of Au-NPs, the leaf extract (0.2, 0.4, 0.6, 0.8 and 1 mL) was added to a vigorously stirred 10 mL of 2×10^{-4} M $HAuCl_4$. $3\,H_2O$ and kept at room temperature to get the colloids gm_1-gm_5. For gm_1 the reduction was slow and completed in 36 h (approximately). The reduction rate is found to increase with increase in the quantity of the leaf extract. For gm_5, fast reduction occurred as indicated by purple pink color of solution (figure 2) and the reaction rate was completed within 4 h. The resulting gold colloid is found to be stable for more than 2 months.

2.5. Characterization of Au-NPs

2.5.1. UV–Vis spectral analysis. The reduction of pure Au^{3+} ions was routinely monitored by visual inspection as well as the optical absorption spectra of biosynthesized Au-NPs. UV-Vis absorption spectrum of the biosynthesized Au-NPs was done in UV-Vis spectrophotometer (Shimadzu UV-1650) in a wave length range from 200 to 800 nm.

2.5.2. Particle size analysis and zeta potential measurements. Particle size (hydrodynamic diameter) and size distribution measurements of the biosynthesized and chemical synthesized Au-NPs were carried out using a Zetasizer, version 6.32 (Malvern Instruments Ltd) based on dynamic light scattering. Stability of biosynthesized nanoparticles was also determined by means of zeta potential analyser using a Zetasizer, version 6.32 (Malvern Instruments Ltd). The measurement of zeta potential is based on the direction and velocity of particles under the influence of known electric field.

2.5.3. Transmission electron microscopy. The size and shape of the particles were measured with high resolution transmission electron microscope (HR-TEM) using Phillips Technai G2 Fei 12 Model equipped with selected area electron diffraction pattern (SAED) operating at an accelerating voltage of 200 kV. A specimen for HR-TEM sample was made by placing a drop of suspension on a carbon coated copper grid and the excess solution was removed by tissue paper and allowed to air dry at room temperature for overnight.

2.5.4. Atomic force microscope. Atomic force microscope (AFM) was used to observe the surface morphology and size of the resultant Au-NPs. The sample was dropped onto new cleaved mica slices and dried overnight. AFM study of the Au-NPs deposited on mica slices was performed in a microscope AGILENT-N9445A series 5500 AFM.

2.5.5. X-ray diffraction. The crystalline characterization of the biosynthesized Au-NPs was conducted with on Bruker AXS D8 Advance X-ray diffractometer operating at a voltage of 40 kV and a current of 30 mA With Cu-Kα radiation ($\lambda = 1.5420$ Å). The scanning range (2θ) was selected from 30° to 80° at a 0.045° min^{-1} continuous speed. The crystallite domain size was calculated through the Debye–Scherrer's formula.

2.5.6. Fourier transform infrared spectroscopy. FT-IR spectroscopy measurements were carried out to identify the possible functional groups of leaf extracts for nanoparticles synthesis and stabilization. FT-IR spectra of the leaf extract and dried biosynthesized Au-NPs were mixed with KBr pellets and recorded with an Avatar 330 FT-IR spectrometer in the range of 4000–400 cm^{-1}.

2.5.7. Screening of anti-bacterial activity. The anti-bacterial activity of biosynthesized Au-NPs, chemically synthesized Au-NPs and crude leaf extract were evaluated against human pathogens such as *Staphylococcus aureus* (gram-positive) and *Vibrio cholera* (gram-negative) by well diffusion method. The selected bacteria were maintained on nutrient agar

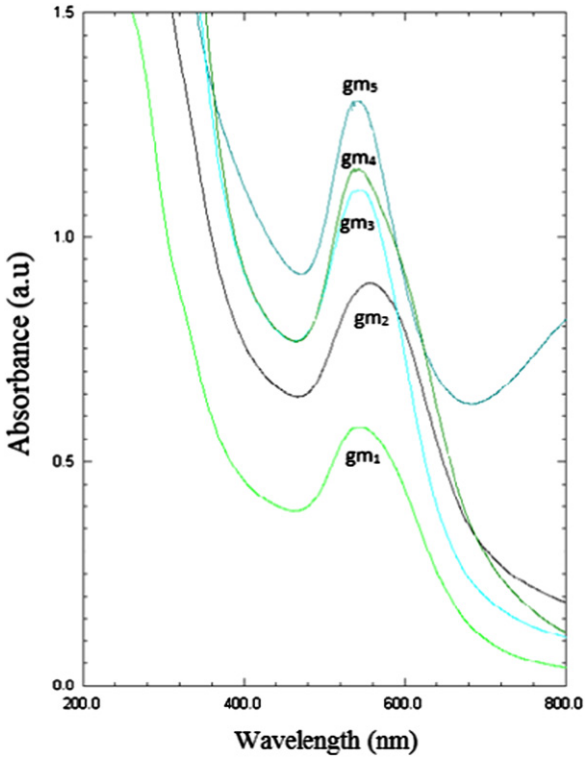


Figure 3. UV-Vis spectra of Au-NPs prepared at different leaf extract concentration (gm_1) 0.2 mL, (gm_2) 0.4 mL, (gm_3), 0.6 mL, (gm_4), 0.8 mL and (gm_5) 1 mL.

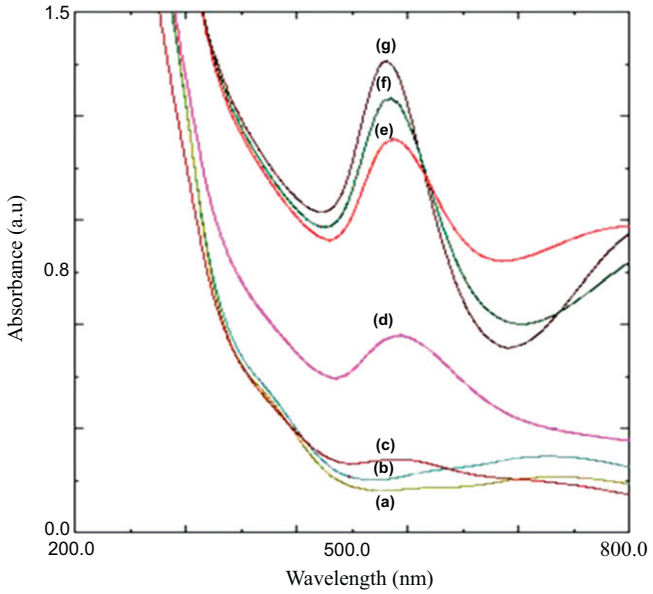


Figure 4. UV-Vis spectra recorded as a function of time of reaction of aqueous solution of chloroauric acid with *Morus alba* (mulberry) leaf extract for gm_5 at time interval of (a) 5 min, (b) 30 min, (c) 1 h, (d) 2 h, (e) 3 h, (f) 4 h, and (g) 24 h.

media. Approximately 7 mm diameter of well was made on Muller Hinton Agar plate with the help of gel puncture. The cultures were swabbed on test media with sterile cotton swab. 50 μL of both chemical and biosynthesized Au-NPs were inoculated to the well, and then the plates were incubated in incubator for 37 °C for 24 h; the zones of inhibition were discussed.

3. Results and discussion

3.1. UV-Vis spectra of Au-NPs

UV-Vis absorption spectroscopy is an important technique to determine the formation and stabilization of biosynthesized Au-NPs in aqueous solution. Colloidal solutions of biosynthesized Au-NPs show a very intense color, which is absent in the bulk material as well as for individual atoms. Color of gold colloid is attributed to surface plasmon resonance (SPR) arising due to the collective oscillation of free conduction electrons induced by an interacting electromagnetic field [32]. Figure 3 shows the UV-Vis spectra of Au-NPs formation using a constant $HAuCl_4$ concentration (2×10^{-4} M) with various concentrations of mulberry leaf extract of (gm_1) 0.2 mL, (gm_2) 0.4 mL, (gm_3) 0.6 mL, (gm_4) 0.8 mL and (gm_5) 1.0 mL aqueous medium. The gradual color change from violet to purple pink color was observed during the reaction with varying concentration of mulberry leaf extract, which are characteristics of the SPR of different size of Au-NPs in solution. Initially, the maximal SPR peaks of Au-NPs showed a broadening in bandwidth of the peak with the decreased concentration of leaf extract (gm_1 is 0.2 mL and gm_2 is 0.4 mL). At higher concentrations, the SPR peak is shifted towards shorter wave length region which shows a decrease in particle size [33]. The broadening in SPR at lower concentrations was probably due to the damping of the SPR caused by the combined effect of an increase in particle size and shape of the Au-NPs in colloidal solutions. Also, at lower concentrations of the leaf extract, nanoparticles syntheses are not greatly favored due to the absence of sufficient biomolecules responsible for capping and efficient stabilization. Further, it is observed that SPR band becomes narrower and finally a sharp absorption peak occurs at 538 nm, which is characteristic of spherical nanoparticles. Thus, from the results it can be inferred that the concentration of extract plays an important role in determining the size distribution of Au-NPs.

Figure 4 shows the UV-Vis spectra of the $HAuCl_4$ solution after the addition of 1 mL (gm_5) of mulberry leaf extract to 10^{-4} M aqueous $HAuCl_4$ resulting in the color change to purple-pink color after 4 h of reaction. The color change in the solution indicates the formation of Au-NPs. Further, it can be observed that the reduction of gold ions reaches saturation after 24 h of reaction, and after that, only slight variations can be noted in the intensity of SPR bands. This result indicates the stability of the nanoparticles for 24 h.

3.2. Particle size and zeta potential measurements

The dynamic light scattering (DLS) analysis is used to measure the shell thickness of a capping or stabilizing agent

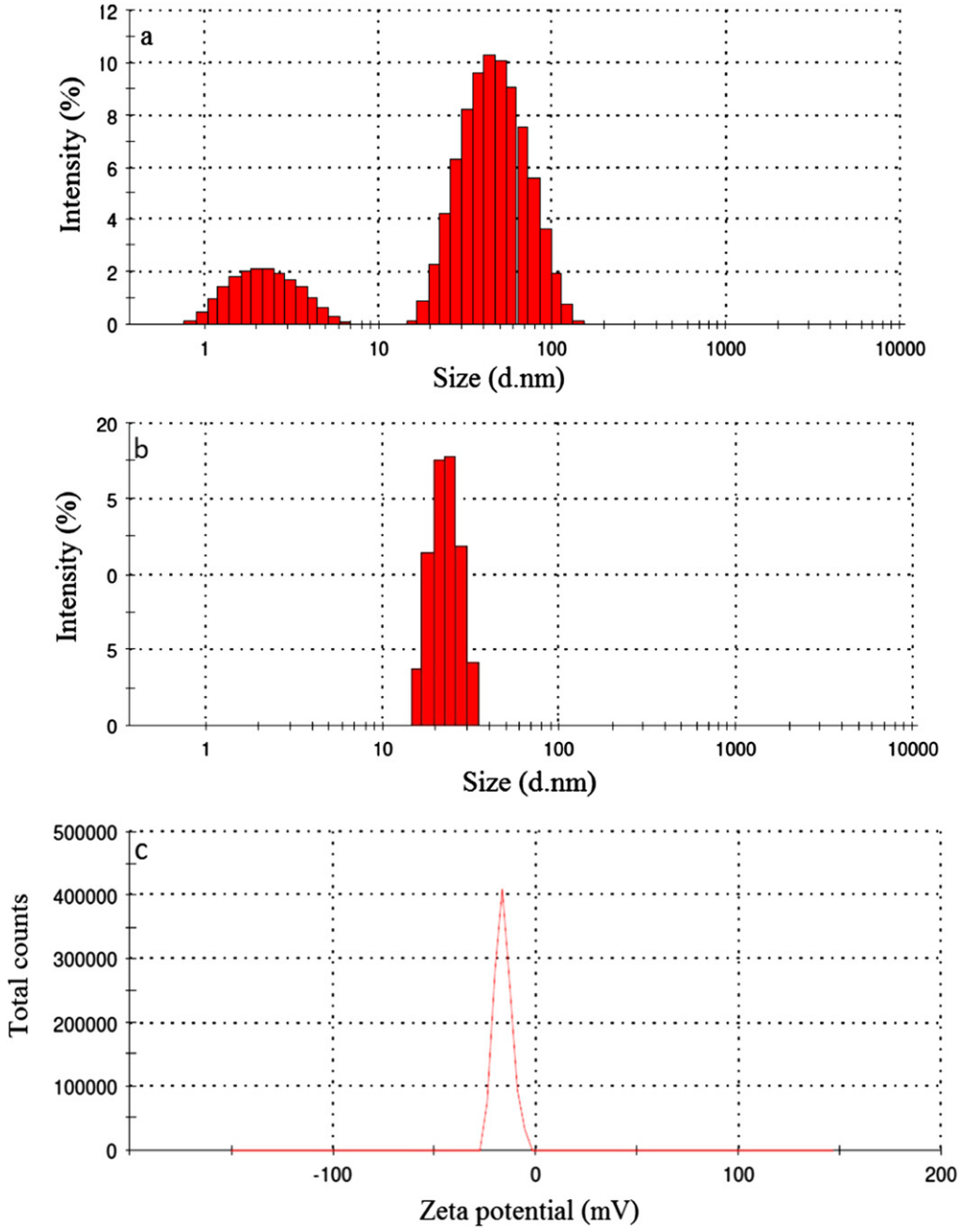


Figure 5. (a) DLS pattern of biosynthesized Au-NPs and (b) of chemical synthesized Au-NPs, (c) zeta potential distribution of biosynthesized Au-NPs.

enveloping the metallic nanoparticles along with the actual size of the metallic core. Figure 5(a) shows the particle size distribution of the biosynthesized Au-NPs using DLS measurements. The average particle size of the Au-NPs was found to be around 50 nm. DLS analysis showed the size distribution of chemical synthesized Au-NPs with maximum intensity at 23 nm (figure 5(b)).

Zeta potential (ZP) values reveal information regarding the surface charge and stability of biosynthesized Au-NPs. Figure 5(c) shows the corresponding average ZP value (−16 mV) suggesting higher stability of colloidal Au-NPs. The rich source of proteins in the mulberry leaf extract may possibly be responsible for reduction of metal ions and efficient stabilization of biosynthesized nanoparticles [34].

3.3. Transmission electron microscope (TEM) analysis

The size and shape of the biosynthesized Au-NPs was further confirmed by TEM analysis. Figures 6(a) and (b) showed that two different magnifications of nearly spherical Au-NPs were synthesized along with a few irregular shaped particles. The particle sizes distributed in the range of 15–53 nm, with an average particle size of 35 ± 6 nm synthesized (figure 6(c)). This large variation in particle size was due to the presence of

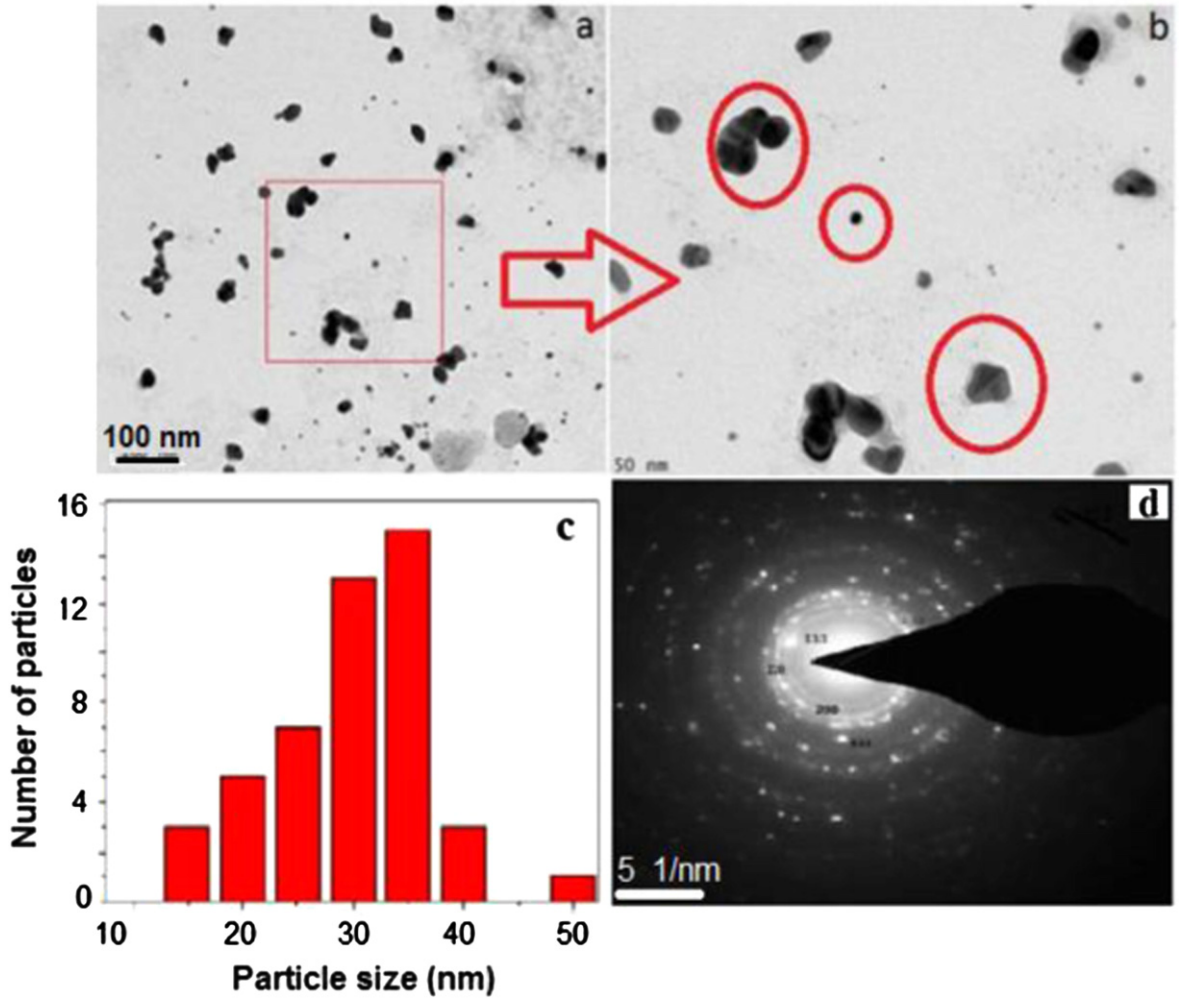


Figure 6. (a) and (b) TEM images of gold colloid (gm_5) at different magnifications, (c) histogram showing the particle sizes of biosynthesized Au-NPs corresponding to TEM images and (d) selected area electron diffraction (SAED) pattern.

a few irregular shaped particles. The nanoparticles appear to be considerably smaller than the average particle size observed with the DLS analyzer, presumably arising from the dry state of the TEM measurements. Also, the large size of particles observed by DLS is due to the fact that the measured size also includes the bio-organic compounds enveloping the core of the Au-NPs. Crystalline nature of the Au-NPs is confirmed by the selected area electron diffraction (SAED) pattern (figure 6(d)) with bright circular spots corresponding to (111), (200), (220) and (311) planes of the fcc lattice of gold [12].

3.4. Atomic force microscopy (AFM) analysis

AFM is an important biophysical technique for studying the morphology of nanoparticles and biomolecules. Figures 7(a) and (b) show the atomic micrograph of biosynthesized Au-NPs with aerial and 3D topographical view of the topological structures. The particle size is in the range below 50 nm. From the topographical view, it is evident that most of the nanoparticles are spherical and have regular shapes. The results observed in TEM images (figure 6) quite agree with the AFM observations results.

3.5. X-ray diffraction (XRD) studies

The crystalline nature of biosynthesized Au-NPs was further confirmed by XRD measurements. Figure 8 shows a representative XRD pattern of the Au-NPs synthesized by the mulberry leaf extract after the complete reduction of Au^{3+} to Au^0. The intense diffraction peak was observed at 2θ values of 38.3° which was indexed to the (111) planes of face-centered cubic (fcc) gold crystals, respectively (JCPDS no. 04-0784). The absence of any other crystallographic impurities and peak broadening in XRD spectrum has confirmed the high purity of synthesized Au-NPs. The peak widths and shapes describe the deviation from a perfect crystal and make clear about the crystalline size if it is less than roughly 100 –200 nm. The width of the most intense reflection (111) peak was employed to calculate the average crystallite size using Debye–Scherrer equation. From the equation, the average crystallite size of Au-NPs found to be around 14 nm. The XRD pattern thus clearly shows that the Au-NPs formed by

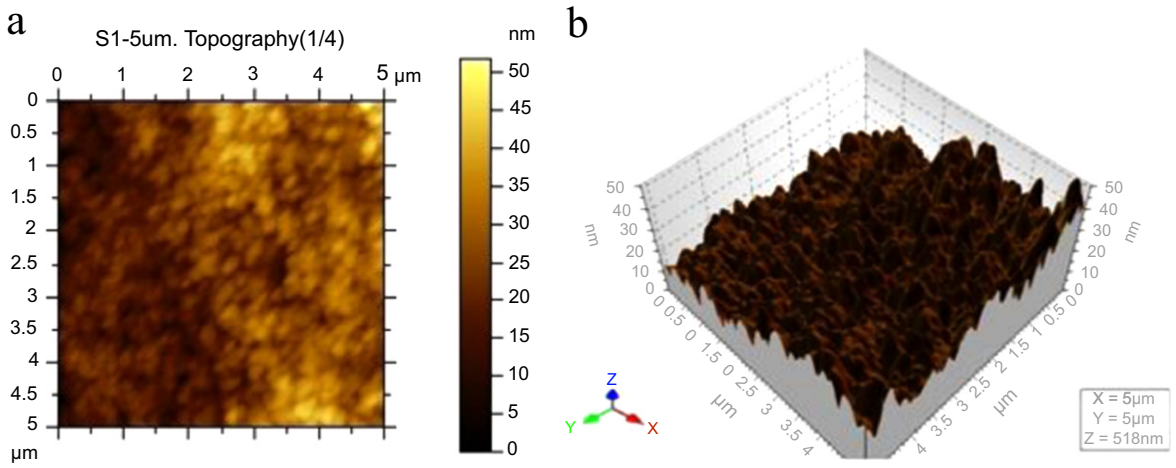


Figure 7. AFM images of biosynthesized Au-NPs. (a) topographic view and (b) three dimensional view.

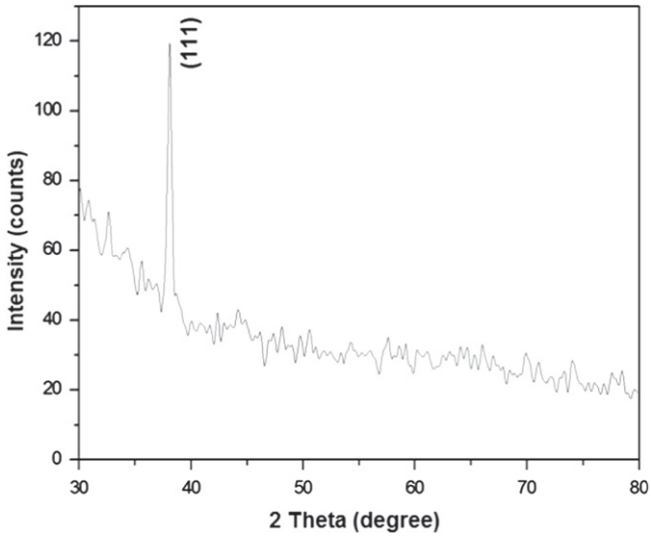


Figure 8. XRD pattern of dried powder of biosynthesized Au-NPs.

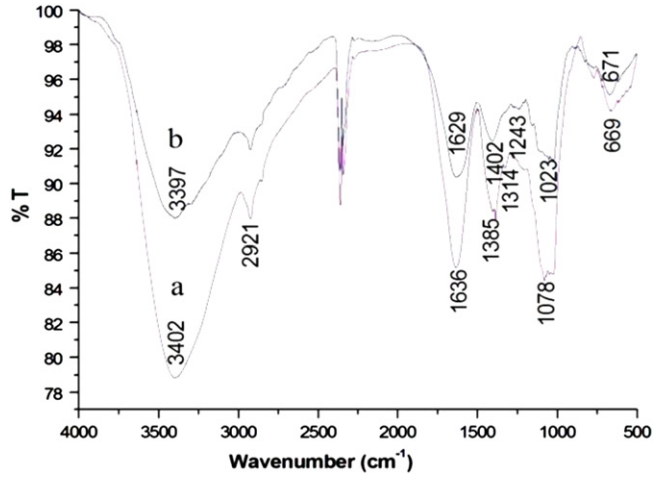


Figure 9. FT-IR spectrum of (a) biosynthesized Au-NPs and (b) *Morus alba* leaf.

the reduction of $AuCl_4^-$ ions by *Morus alba* leaf extract are crystalline in nature.

3.6. Fourier transform infrared spectroscopy (FT-IR) spectroscopy

FT-IR measurements were carried out to identify the possible biomolecules responsible for capping and efficient stabilization of the Au-NPs synthesized using mulberry leaf extract. Curves a and b in figure 9 show the FT-IR spectra of biosynthesized Au-NPs and leaf extract of *Morus alba*, respectively. The biosynthesized Au-NPs show intense bands at 3402 cm^{-1}, 2920 cm^{-1}, 1636 cm^{-1}, 1385 cm^{-1} 1078 cm^{-1}, 1023 cm^{-1} and 669 cm^{-1}. This represents different functional groups of adsorbed biomolecules on the surface of the nanoparticles and also indicates the influence of organic moieties on the formation of Au-NPs and for stabilization in the aqueous medium. The strong band observed at 3402 cm^{-1} corresponds to the amine group stretching vibrations super imposed on the side of hydroxyl group [14]. The peak at 2920 cm^{-1} could be assigned to C–H stretching vibrations of methyl, methoxy and methylene groups [20]. The band observed at 1636 cm^{-1} is identified as the amide I and arises due to the carbonyl stretch vibrations in the amide linkages of the proteins. [32, 33] The band observed at 1385 cm^{-1} was assigned to C–N stretching [20]. The peaks at 1078 cm^{-1} and 1023 cm^{-1} are the characteristics of C-OH vibrations of proteins and –C–O–C bending mode, respectively. [33, 35] The band at 669 cm^{-1} might be the plane bending vibrations N-H groups of proteins [36]. The presence of secondary metabolites such as flavonoids, phenols, aminoacids and anthocyanins was reported in *Morus alba* leaf extract [27]. Figure 9 showed variations in the band position and band intensity due to the reduction of Au^{3+} ions to Au^0. Curve a in figure 9 shows slight shifts along with increase in the intensites at 3402 cm^{-1} and 1636 cm^{-1}, respectively, and reveals the binding of a (NH)C=O group with Au-NPs. Curve a also shows increased band intensities at 1023 cm^{-1} and 669 cm^{-1} as compared to curve b in figure 9 and suggests that synthesized Au-NPs were stabilized by negatively charged aminoacid molecules.

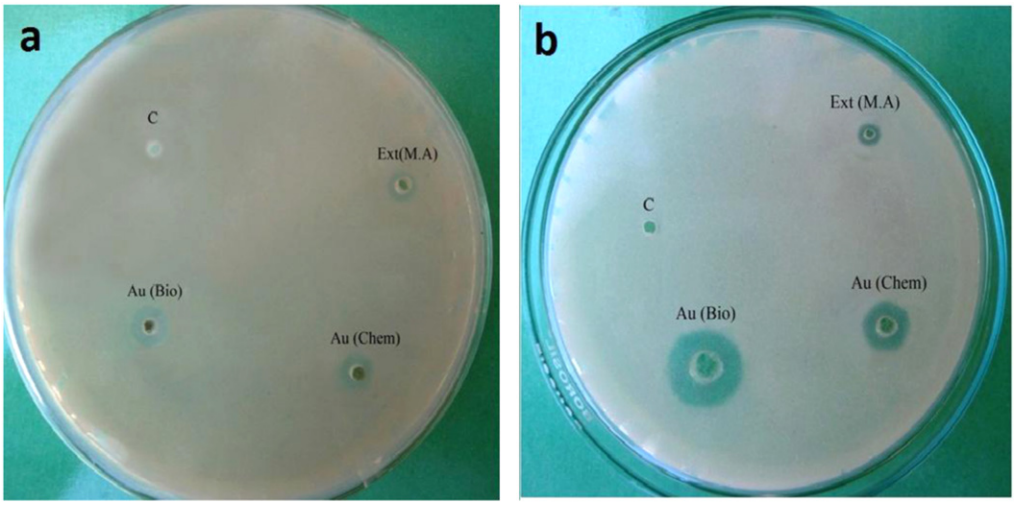


Figure 10. Anti-bacterial assay of *Morus alba* extract, biosynthesized Au-NPs and chemical synthesized Au-NPs using well diffusion test against *Staphylococcus aureus* (a) and *Vibrio cholera* (b).

Table 1. Inhibitory action of control, *Morus alba* leaf extract, chemically synthesized Au-NPs and biosynthesized Au-NPs against human pathogenic bacteria.

	Inhibition zone (mm)			
Bacterial species	Control	Leaf extract (30 μm)	Au-NPs (chem.) (50 μm)	Au-NPs (chem.) (50 μm)
Vibrio cholera	—	6	15	25
Staphylococcus aureus	—	5	11	13

3.7. Antibacterial activity of gold nanoparticles

In the present study, anti-bacterial activity of biosynthesized Au-NPs, chemical synthesized Au-NPs and aqueous leaf extract were tested against two human pathogens such as *Staphylococcus aureus* (gram-positive) and *Vibrio cholera* (gram-negative) at the concentration of 50 μl by well diffusion method (figures 10(a) and (b)). The diameter of inhibition zones (mm) around each well with biosynthesized Au-NPs, chemical synthesized Au-NPs and aqueous leaf extract were represented in table 1. The Au-NPs synthesized by *Morus alba* leaf extract were found to be highest anti-bacterial activity against *Vibrio cholera* and moderate inhibition against *Staphylococcus aureus*. Chemical synthesized Au-NPs exhibit very fair activity against *Staphylococcus aureus* and *Vibrio cholera.* The lesser anti-bacterial activity of aqueous leaf extract was found against *Staphylococcus aureus* and *Vibrio cholera*. The accumulation of gold ions on the negatively charged cell membrane of *Vibrio cholera* leads to conformational changes in cell membrane, which loses permeability control which in turn causes the cell death [37]. This result is possible due to difference in the structure of the cell wall between gram-positive and gram-negative bacteria. The cell wall of the gram-positive bacteria is composed of a thick layer of peptidoglycan, consisting of linear polysaccharide chains cross-linked by short peptides thus forming more rigid structure leading to difficult penetration of the Au-NPs compared to the gram-negative bacteria where the cell wall possesses a thinner layer of peptidoglycan [38]. Biosynthesized Au-NPs, showed efficient anti-bacterial activity compared to chemical synthesized Au-NPs due to their capping agents (mulberry proteins) and it has great potential to kill the pathogens.

From the present results, it is clearly evident that the higher inhibitory action of biosynthesized Au-NPs depends not only on size of the nanoparticles, but also on the capping agent (proteins) of the nanoparticles. The surface charge and chemical properties of NPs are determined by capping agents, which play an important role during NPs and bacterial interactions.

4. Conclusion

The present work reports a simple, novel and successful synthesis of gold nanoparticles using *Morus alba* leaf extract as a novel reducing and stabilizing agent of gold salts. UV-Vis spectral analysis confirmed the surface plasmon resonance of biosynthesized Au-NPs. The DLS HR-TEM and AFM images studies had shown that the synthesized Au-NPs have a size below 60 nm. Zeta potential value for biosynthesized Au-NPs was −16 mV indicating the stability of the nanoparticles. Crystalline nature of the nanoparticles is evident from bright circular spots in the SAED pattern and characteristic peak in the XRD pattern. From FT-IR spectra, it was found that biomolecules responsible for capping and stabilization of Au-NPs were water soluble proteins present in the mulberry leaf extract. Moreover, anti-bacterial activity of biosynthesized Au-NPs showed better activity towards gram-

negative *Vibrio cholera* than gram-positive *Staphylococcus aureus* compared to chemically synthesized Au-NPs. The development of such plant materials mediated synthesis of Au-NPs can be used as a good therapeutic agent against human and veterinary pathogens and also for the successful development of drug delivery in the near future.

Acknowledgements

The authors are grateful to the authority of Annamalai University for providing all necessary facilities to carry out the present work.

References

[1] Tamura M and Fujihar H 2003 *J. Am. Chem. Soc.* **125** 15742
[2] Jia L, Zhang Q, Li Q and Song H 2009 *Nanotechnology* **20** 385601
[3] Jain P K, Huang X, El-Sayed I H and El-Sayed M A 2008 *Acc. Chem. Res.* **41** 1578
[4] Liu Y, Hu J, Kong Q and Feng X 2010 *Mater. Lett.* **64** 422
[5] Leng C, Wu J, Xu Q, Lai G, Ju H and Yan F 2011 *Biosens. Bioelectron.* **27** 71
[6] Philip D 2010 *Spectrochim. Acta* A **77** 807
[7] Sadhasivam S, Shanmugam P and Yun K 2010 *Colloids Surf.* B **81** 358
[8] Jebakumar I E T and Sethuraman M G 2012 *Process Biochem.* **47** 1351
[9] Aswathy A S, Vidhu V K and Philip D 2012 *Spectrochim. Acta* A **85** 99
[10] Dwivedi A D and Gopal K 2010 *Colloids Surf.* A **369** 27
[11] Philip D and Unni C 2011 *Physica* E **43** 1318
[12] Ganesh K V, Dinesh G S, Rajeswari A, Stalin D T, Karthick V, Kapadia Z, Shrestha T, Barathy I A, Roy A and Sinha S 2011 *Colloids Surf.* B **87** 159
[13] Noruzi M, Zare D, Khoshnevisan K and Davoodi D 2011 *Spectrochim. Acta* A **79** 1461
[14] Vijayakumar R, Devi V, Adavallan K and Saranya D 2011 *Physica* E **44** 665
[15] Ghoreishi S M, Behpour M and Khayatkashani M 2011 *Physica* E **44** 97
[16] Noruzi M, Zare D and Davoodi D 2012 *Spectrochim. Acta* A **94** 84
[17] Mohan K K, Kumar M B, Sinha M and Krishnakumar V 2012 Spectrochim *Acta* A **86** 490
[18] Ankamwar B, Chaudhary M and Sastry M 2005 *Synth. React. Inorg. Metal Org. Nano Met. Chem* **35** 19
[19] Govindaraju K, Kiruthiga V, Manikandan R, Ashokkumar T and Singaravelu G 2011 *Mater. Lett.* **65** 256
[20] Ashok B, Bhagyashree J, Ameeta R and Smita Z 2010 *Colloids Surf.* B **80** 45
[21] Daisy P and Saipriya K 2012 *Int. J. Nanomed.* **7** 1189
[22] Sudip M, Vinothkumar B, Suthari P, Prakriti R B, Bojja S and Chitta R P 2013 *RSC Adv.* **3** 2318
[23] Praveen K K, Paul W and Sharma C P 2011 *Process Biochem.* **46** 2007
[24] Mohammed F A, Girilal M, Venkatesan R and Kalaichelvan P T 2011 *Colloids Surf.* B **88** 287
[25] Srivastava S, Kapoor R, Thathola A and Srivastava R P 2006 *Int. J. Food Sci. Nutr.* **57** 305
[26] Tzi-Peng Y, Huei-Jane L, Ting-Tsz O, Ya-Ju C and Chau-Jong W 2012 *J. Agric. Food Chem.* **60** 6891
[27] Sadiqbutt M, Nazir A, Tauseef S M and Schroen K 2008 *Trends Food Sci. Technol.* **19** 505
[28] Chan K C, HO H H, Peng C H, Lan K P, Lin M C, Chen H M and Wang C J 2010 *J. Agric. Food Chem.* **58** 2536
[29] Asano N, Yamashita T, Yasuda K, Ikeda K, Kizu H, Kameda Y, Kato A, Nash R J, Lee H S and Ryu K S 2001 *J. Agric. Food Chem.* **49** 4208
[30] Toshiyuki K, Kiyotaka N, Hiroyuki K, Yoshihiro K, Yuko G, Kenji Y, Shigeru O, Shinichi O and Teruo M 2007 *J. Agric. Food Chem.* **55** 5869
[31] Lee B T and Ranville J F 2012 *J. Hazard. Mater.* **213** 434
[32] Jayaseelan C, Rajendiran R, Abdul A R and Pachiappan P 2013 *Industrial Crops Prod.* **45** 423
[33] Aswathy A S and Philip D 2012 *Spectrochim. Acta* A **97** 1
[34] Sukirtha R, Priyanka K M, Antony J J, Kamalakannan S, Thangam R, Gunasekaran P, Krishnan M and Achiraman S 2012 *Process Biochem.* **47** 273
[35] Sheny D S, Mathew J and Philip D 2011 *Spectrochim. Acta* A **79** 254
[36] Aswathy A S and Philip D 2012 *Physica* E **44** 1329
[37] Ramamurthy C H, Padma M, Daisy mariya samadanam I, Mareeswaran R, Suyavaran A, Suresh K M, Premkumar K and Thirunavukkarasu C 2013 *Colloids Surf.* B **102** 808
[38] Kaviya S, Santhanalakshmi J, Viswanathan B., Muthumary J and Srinivasan K 2011 *Spectrochim. Acta* A **79** 594